A Study on Coastal Flooding and Risk Assessment under Climate Change in Mid-Western Coast of Taiwan

Tai-Wen Hsu[1], Dong-Sin Shih[2]*, Chi-Yu Li[3], Yuan-Jyh Lan[4], Yu-Chen Lin[5]

[1]Department of River and Harbor Engineering, National Taiwan Ocean University, Taiwan; Email: twhsu@mail.ntou.edu.tw

[2]Department of Civil Engineering, National Chung Hsing University, Taiwan; Email: dsshih@nchu.edu.tw

[3]Institute of Marine Environment and Ecology, National Taiwan Ocean University, Taiwan; Email: chiyuli@ntou.edu.tw

[4]Center of Excellences for the Oceans, National Taiwan Ocean University, Taiwan; Email: yjlan@mail.ntou.edu.tw

[5]Center for Research in Water Science and Technology, National Cheng Kung University, Taiwan. Email: shuchen@mail.ukn.edu.tw

*Corresponding author: Shih Dong-Sin

Department of Civil Engineering, National Chung Hsing University, No.145, Xingda Rd., South Dist., Taichung City 402, Taiwan; PH +886-4-22872221 ext.308; Email: dsshih@nchu.edu.tw

Abstract

This study integrated coastal-watershed models and combined a risk assessment method to develop a methodology to investigate the impact resulting from coastal disasters under climate change. The mid-western coast of Taiwan suffering from land subsidence was selected as the demonstrative area for the vulnerability analysis based on prediction of sea level rise (SLR), wave run-up, overtopping, and coastal flooding under the scenarios of 2020 to 2039. Database from tidal gauges and satellite images were used to analyze sea level rise using EEMD (Ensemble Empirical Mode Decomposition). Extreme wave condition and storm surge were estimated by numerical simulation using WWM (Wind Wave Model) and POM (Princeton Ocean Model). Coastal inundation was then simulated via WASH123D watershed model. The risk map of study areas based on the analyses of vulnerability and disaster were established using the AHP (Analytic Hierarchy Process) technique. Predictions of sea level rise, the maximum wave condition and storm surge under the scenarios of 2020 to 2039 are presented. The results indicate that the sea level at the mid-western coast of Taiwan will rise in an average of 5.8 cm, equivalent to a rising velocity of 2.8 mm/year. The analysis indicates that Wuqi, Lukang, Mailiao, and Taixi townships are susceptive, low resistant and low resilient, and reaches the high risk level. The assessment

provides that important information for making adaption policy in the mid-western coast of Taiwan.

Keywords: Climate Change; Coastal Disasters; Vulnerability; Disaster Risk.

1. Introduction

"Climate Change" has been one of the most concerned issues in the natural science field. The 2015 United Nations Climate Change Conference (COP 21) was held in Paris, France, and the Paris Agreement was signed by participating countries on the reduction of climate change. The Intergovernmental Panel on Climate Change (IPCC) also has its Fifth Assessment Report (AR5) (https://www.ipcc.ch/report/ar5/) pointing to the trend of the latest global climate change with warnings. The report concludes that lots of natural systems are being negatively affected by regional climate changes from most observed continental and marine evidences (IPCC, 2014). The estimation average global flood losses are approximately US$6 billion per year, increasing to US$52 billion by 2050 with projected socio-economic change alone (Hallegatte *et al.*, 2013). Recent studies concluded that climate scenarios from General Circulation Models (GCMs) or Regional Climate Models (RCMs) are the largest uncertainty for estimation of future flows (Déqué *et al*., 2007; Menzel *et al*., 2006; Minville *et al*., 2008; Prudhomme and Davies, 2008). More Researches have further to point that climate change is evidenced to affect local rainfall amounts, surface runoffs and distribution

of water resources (Akhtar *et al*., 2008; Arnell and Gosling, 2013; Guo *et al.*, 2002; Kling *et al.*, 2014). That is typically characterized by shifts in temperature and precipitation, which are in response to their regions specific, e.g. alteration of extremes, intensities, frequencies, spatial and temporal patterns (Easterling *et al.*, 2000; Hay *et al.*, 2011; Hovenga *et al.*, 2016). Climate change alters the risk of hydrological extremes at regional scales, and their hydrological response of a catchment can vary substantially not only due to its location but also depending on the characteristics of the catchments (Acreman and Sinclair, 1986; Beven *et al*., 1988; Veijalainen *et al*., 2010; Yan *et al*., 2015).

During the past fewer decades, the upward historical trends of sea level rise (SLR) quantified from a small set of California tide gauges to a value approximately 20 cm/century. That is quite similar to the estimated value of global mean sea level (Cayan *et al.*, 2008). It attributed primarily to global climate change and associated with their land situations (Cayan *et al.*, 2008; Mastrandrea and Luers, 2012; Rahmstorf, 2007; Scavia *et al.*, 2002). So using dynamic modeling framework to examine the effects of global climate change, and SLR in particular, on tropical cyclone-driven storm surge inundation is implemented (Bilskie *et al.*, 2014; Bilskie *et al.*, 2016; Hovenga *et al.*, 2016; Passeri *et al.*, 2015; Passeri *et al.*, 2016). Most of people who estimated flooding in 2100 is 16–388 million for the mid (55-cm) global-mean SLR scenarios, and up to

510 million people/year for the high (96-cm) scenario (Nicholls, 2002). On northern Gulf of Mexico, the total inundated land area increases by 87% and peak surge increase by as much as 1 m above the applied SLR in some areas, and other regions were subject to a reduction in peak surge, with respect to the applied SLR, indicating a nonlinear response (Bilskie *et al.*, 2016). Passeri *et al.* (2016) addressed that tidal amplitudes within the bays increased 67% of 10.0 cm under the highest SLR scenario, and the ratio of the maximum flood to maximum ebb velocity decreased in the future scenarios by 26% and 39%. Bilskie *et al.*, (2014) showed that the storm surge response to SLR is dynamic and sensitive to changes in the landscape. Hovenga *et al.* (2016) presented the effects of climate change on overland processes, river inflow, and, sediment loading for the Apalachicola region. To the same region, Chen *et al*. (2014) reported that the seasonal response of runoff and sediment loads are slight with contrasting behaviors from different models. But flow increased from the baseline by 8% using model simulation. Previous researches have shown that tidal flows and storm surge dynamics really depend on future SLR scenarios (Bilskie *et al.*, 2016; Passeri *et al.*, 2015; Passeri *et al.*, 2016).

Taiwan is located at the hub of the typhoon route in the west Pacific Ocean, and frequently struck by typhoons and tropical depressions with raging storms and pouring rains during summer and autumn seasons. According to past century typhoon records

from the Central Weather Bureau (CWB) in Taiwan, there are in average 4.0 typhoons per year attacking Taiwan. It is also noted that the strength and the scale of a typhoon increase with the decreased center pressure during recent 14 years. This brings about heavy rains, big waves, storm surges, and floods in the coastal areas. The related long term observations indicated that the SLR increases at a speed of 3.32 mm/year (Beckley *et al.*, 2007; Wu *et al.*, 2011; Bilskie *et al.*, 2014). Statistics of historical data from different stations also confirms the increasing rising trend. A global rate of 3.36 ± 0.41 mm/yr over the 14 years from 1993 to 2007 is investigated, but the regional sea level trend comparisons for the time periods of 1993–1999 and 1999–2005 reveal strong basin-scale polarities and pronounced inter-decadal variability, with a relative increase in the global mean SLR trend of 1.5 ± 0.7 mm/yr in the latter seven years (Beckley *et al.*, 2007). Water level changes due to storm surges and high tides resulting from typhoons often cause severe disaster to the coastal areas of Taiwan (Hsu *et al.*, 2015). The storm surges and high tides directly striking the coasts bring about serious beach erosion and waves overtopping the seawall to cause seawater intrusion and floods in the coastal areas. These damage the crops, the fishing farms, life and properties. They also make colossal negative impact on the development of marine environment in Taiwan (Hsu *et al.*, 2015). The assessment of the possible impact of climate changes could help us to make appropriate strategies

for remediation and prevention. To classify risk levels, Analytic Hierarchy Process (AHP) method was used to identify flood hazard of risk assessment (Stefanidis and Stathis, 2013; Tehrany *et al*., 2014).

Large populations live in the coastal areas where they are exposed to a range of hazards including coastal flooding (Small *et al.*, 2000; Small and Nicholls, 2003). The basic model used to predict flood impacts has already been outlined by earlier studies (Nicholls *et al.*, 1999, Nicholls, 2004). This study aims to investigate the coastal adaptability to climate change related disasters. A methodology integrating coastal-watershed models and a risk assessment method was developed to investigate such impact on coastal areas. The mid-western coast of Taiwan was selected as the demonstrative site to test the approach. The final results of this methodology would produce risk maps which were derived from the results of analyses of vulnerability and hazard under the scenarios. The map could provide important information for engineers to make adaptation in Taiwan.

2. Methodology

2.1 Coastal Risk Assessment

Humans living in the coastal areas are often prone to the impact from storms, sea waves and tides, and SLR. To make it worse, the present situations of global warming and climate change have made the SLR problems more conspicuous. Therefore, a

Preprints (www.preprints.org) | NOT PEER-REVIEWED | Posted: 21 March 2017 doi:10.20944/preprints201703.0172.v1

Peer-reviewed version available at Water 2017, 9, , 390; doi:10.3390/w9060390

systematic approach to assess the risk, including overall vulnerability and disaster analyses, becomes a necessity. The United Nations Disaster Relief Organization (UNDRO) in its 1979 report on Natural Disaster and Vulnerability Analysis (UNDRO, 1980) made an operational definition for the disaster risk, which is the multiplication of hazard potential and vulnerability.

As above mentioned, the final results of risk analysis are represented by digital maps, which are overlapped by different hazard and vulnerability indexes, see on Table 1. These indexes consist of 4 Coastal Hazard Indexes (CHIs) and 13 Coastal Vulnerability Indexes (CVIs). Each index in this study is to be categorized into five different levels represented by five different points, i.e. very low (1 point); low (2 points); medium (3 points); high (4 points); very high (5 points). These values provide a quantitative indicator to assess the risk. A detailed description of these indexes and how the points are assigned will be explained later. The Analytic Hierarchy Process (AHP) was employed to evaluate the risk with following equations:

$$I_{i,j}^{*} = \frac{I_{i,j} - \min\{I_{i,j}\}}{\max\{I_{i,j}\} - \min\{I_{i,j}\}} \quad (1)$$

$$C_i = \sum_{j=1}^{J_i} w_{i,j} \times I_{i,j}^{*} \quad (2)$$

$$R = \sum_{i=1}^{4} w_i^{'} \times C_i \quad (3)$$

where $I_{i,j}$ is the index of j^{th} CHI or CVI in the i^{th} domain, $I_{i,j}^{*}$ is the normalized index determined by the maximum and minimum $I_{i,j}$, C_i is the constructor of the i^{th}

domain by the weighted sumation with the weight $w_{i,j}$, R is the risk defined by the weight $w_i^{'}$.

The Geographic Information System (GIS) was utilized for calculation, analysis and display. The AHP calculation decomposes problems into simple hierarchical frameworks. Each layer of the framework is then searched for its key factors whose order of precedence or contributions are evaluated. And then, the results are overlapped together and processed into the final order of precedence of each project (factor). Details of the AHP process can be referred to Lin and Tang (2003).

According to Lan *et al*. (2013), coastal hazard potential consists of four indexes which are associated with storm surges and floods in coastal areas caused by typhoons. Considering the specific threads of typhoons in Taiwan, the overflow in coastal areas results from the combined impact of precipitation, sea level rise, storm surge, wave setup, wave run-up and overtopping. For describing the overflow as well as determining each CHI, the integrated coastal-watershed models were employed in this study. The results of these models provide the important information of range and depth of coastal flooding. The weight of each index is surveyed by the questionnaires from 100 experts and scholars with different major fields including ocean engineering, hydraulic engineering, and coastal engineering, and so on. The weight of each index is presented in Table 1. Besides, due to these vulnerable coastal areas, especially during

the typhoon seasons, the weights of hazard indexes are higher than those of vulnerability indexes to reflect the seriousness of the problem.

The CVIs are indicators of a region with specific weakness exposed to natural disasters and the capability of coping with it. The concept of coastal vulnerability was firstly proposed by the Coastal Zone Management (CZM) of International Plant Protection Convention (IPPC) in 1991. The coastal vulnerability defined in this study refers to the potential coastal disasters which are caused in the process of flooding or SLR resulting from climate change-related stormy rains. By referring to related researches (e.g. Doukakis, 2005; UNEP, 2005; Hong *et al*., 2006; Kumar and Tholkappian, 2006), as well as the consideration of domestic status quo and data availability, 13 coastal vulnerability indicators were established within the constructs of artificial facilities, environmental geography, and social economy. Within these 13 indicators, the relative ratios of seawall length, seawall height, and tidal gates belong to the construct of artificial facility, which refers to the protection facilities of the hydraulic engineering structures. The coastal elevation, slopes, tidal range, land subsidence rate, coastal erosion rate, and land uses, e.g. harbors, industrial zones, agricultural areas, national parks, etc., belong to the environmental geography. The population density, education background, dependency ratio, and enterprise return are considered as the construct of social economy. The weights of indicators were also

derived from the surveys of 100 experts and scholars in different disciplines, and they are also listed in Table 1. It is noted that the environmental geography domain is weighted at 0.548, which is higher than other values and indicates significant environmental problems.

2.2 Integrated Coastal-Watershed Models

Coastal inundations due to wave overtopping of coastal structures and storm surges often cause serious damage to the populations. Ascertaining the areas that are prone to coastal inundation is essential to provide countermeasures for mitigation of the disaster. Integrated POM-WWM-WASH123D models (Hsu *et al.*, 2015) were employed for simulating the inundation areas of different scenarios. The Rankin Vortex Model (RVM) (Holland, 1980) was used to generate wind fields for the study area. Wave run-up and overtopping were also simulated based on the Reynolds averaged Navier-Stokes (RANS) equations with the particle level set method (Hsu *et al.*, 2005). Different techniques, including Ensemble Empirical Mode Decomposition (EEMD) (Wu *et al.*, 2011) and Fast Fourier Transformation (FFT), were applied to analyze the SLR of future scenarios. The upstream precipitation, estimated by time and space with a designed rainfall pattern which is based on the "Hydrological Design Application Manual" published by the Water Resource Agency (WRA) of Taiwan with long-term and short-term delays (Shih *et al.*, 2012). These provided initial and boundary

conditions for the Integrated POM-WWM-WASH123D models to simulate the overland flow floods in the coastal areas and the hazard maps of the future climate scenarios.

The integrated POM-WWM-WASH123D models are briefly introduced as follows. POM (Princeton Ocean Model) was developed by (Blumberg and Mellor, 1987), and widely used to the study of oceanographic problems. It has been used to simulate the interactions between tides and ocean waves at the estuaries. The POM has been shown to be capable of simulating flow characteristics near estuaries. A more complete discussion of the theoretical bases and development of POM can be found from public document (Mellor, 1998) or the home page at (http://www.aos.princeton.edu/WWWPUBLIC/htdocs.pom). The WWM (Wind Wave Model) was developed by Hsu *et al.* (2011), for describing the processes of wave generation, refraction and diffraction, dissipation and nonlinear wave-wave interactions. Data assimilation techniques were also included to improve the applicability of the sequential simulation. WASH123D stands for Watershed Systems of 1D Stream-River Network, 2D Overland Regime, and 3D Subsurface Media and is an integrated multimedia, multi-process, physics-based computational model used for descripting watershed scale hydrology (Yeh *et al.*, 2006). It also includes the flows of dendritic river/stream/canal networks, overland regimes and subsurface media. Both

river and overland modules are solved using the finite element approach (Yeh *et al.* 2011). In this study, WASH123D was employed for simulating surface routing to estimate the flood regions of the coast. The downstream boundary conditions are imposed on the basis of the surging tides as well as the overtopping. The upstream boundary conditions are then specified by the precipitation. More details of POM-WWM-WASH123D models include description, calibration, validation and application can be founded in previous studies (Shih *et al.*, 2012; Hsu *et al.*, 2015).

3. Application Area, Future Scenarios and Results

3.1 Application Area

As shown in Fig. 1, the mid-western coast of Taiwan, where Taichung City, Changhua County and Yunlin County locate, were selected as the demonstrative site. The Da-an River, Dajia River, Wu River, Jhuoshuei River, and Beigang River are major rivers flowing through these areas. The Taichung coast is mainly situated between the Da-an River and the Wu River and its length is about 41 km. The area near the Da-an River and the Dajia River is estuarine alluvial plain, featured with large tidal ranges and well developed tidal flat and a famous wetland. In addition, this coastal area is suffering severe disasters in early times due to extremely storm surges, huge wave and flat terrain. The Changhua coast is mainly located between the Wu River and Jhuoshuei River having a total length of about 61km. The supply of sediments from the Wu River

and Jhuoshuei River and part of Dajia River produces the alluvial plain. The beach slope is so mild that the tidal flat is broad with several kilometers exposed during the ebb tide.

The Yulin coast located between the Jhuoshuei River and Beigang River, has a total coastal length of about 55 km. A segment of this coast was protected in early stage by the offshore sandbank barriers from the surge invasion. However, the coastal erosion is even more serious and the beach diminished in the further south areas according to the surveys by WRA. This is due to the reduction of the sand supply for the shortage of offshore sandbank barriers attacked by typhoon waves and storm surges. Moreover, severe land subsidence has been observed in recent years causing difficulties in inner drainage. These areas are prone to severe floods, but the situation has been improved due to the mitigation measures by WRA since 2005.

3.2 Coastal Assessment under Climate Changes

For the purpose of studying and assessing the coastal flooding and risk under climate change in mid-western coast of Taiwan, a status quo investigation and data collection on different aspects, including engineering, socioeconomics, land uses, geology, disaster prevention facilities, etc., was carried out. Based on the collected information and the availability of the data, the analysis periods are 1980–1999 for base years and 2020–2039 for scenario years representing the near future. The period

is referred to the classification of platform of Taiwan Climate Change Projection and Information Platform Project (TCCIP). The TCCIP is coordinated by National Science and Technology Center for Disaster Reduction (NCDR), which is one of three major climate change projects funded by Ministry of Science and Technology. The TCCIP project not only produces climate change data for impact assessments and adaptations but also aims to support national adaptation policy frameworks (TCCIP, 2016), which years of 1980-1999 is treated as base time and years of 2020–2039 is defined as near future. The astronomical tides, stormy surges, typhoon waves deriving nearshore wave setup, wave run-up and overtopping of future scenario are then predicted for coastal flooding and risk analysis.

According to the database of Central Weather Bureau (CWB) in Taiwan, the yearly average of minimum typhoon low pressures from 1980 to 1999 is 921.55 hPa, which is treated as the status quo value of atmospheric pressure of typhoons striking Taiwan. The extreme low pressure value of 846 hPa, occurred in year 1961, was recommended by the WRA in Taiwan as the designed atmospheric pressure intensity for scenario years. WWM was used to simulate the maximum typhoon-induced wave heights and the maximum storm surge deviations. According to Lan *et al*. (2013) data measured from Changhua coastal waters has been shown almost to obey Weibull distribution for the extreme value analysis. The exceeding probability that the event is less than 10 %

is proposed for the estimation of wave height and storm surge in the target future. Different maximum wave height and storm surge deviations of different return periods (5 years, 50 years, 100 years, 200 years and 250 years) for the target's future were then derived, and some of them listed in Table 2 and Table 3, respectively. Table 4 also presents the amount of overtopping of different return periods at some major seawalls for the target's future. The maximum wave height induced by typhoons will increase 35.98% (about 2.55 meters) on average, the maximum typhoon surge deviation will increase 29.15% (about 0.28 meters) on average. We further to check the results with stations measurement at Northern Taiwan. For instance, Figs. 2 and 3 show the rapid increasing trend of maximum wave height measured at Long Dong station and maximum annual surge level at Fugan station respectively. An inspection of Figs. 2 and 3, it is noticed that the increasing rate is sometimes higher than 45% for some periods.

Above results provide a database to fit the assumption that the offshore waves hit the near-shore seawalls in the right front. The simulations of the impact on wave run-up and overtopping for the status-quo year of 2014 and the scenarios from years 2020 to 2039 were performed. The simulated results show the surging tides (astronomic tides superposed with surging tide deviations) of different recurrence periods and the sea level rising volumes of the target years. The sea level rising volume of 6.0 cm at

the Taichung Harbor is chosen as the reference level for the model simulation. The average wave overtopping volumes of all the major seawalls were conducted. The results indicated that most of seawalls have small amount of wave overtopping except for the Shingong seawall in Kouhu Township of Yulin County.

Two different techniques, FFT and EEMD, were utilized to analyze the SLR for the target's future. The estimation of average SLR at Taichung Harbor and Dongshi tidal stations are summarized in Table 5. The average amount of sea level rise is in the range of 5.2 cm to 6.2 cm from 2020 to 2039, and equivalent to rising velocity approaches to 2.8 mm/year. The comparison of analysis from the Taichung Harbor and Dongshi tide-gauge station of Chiayi County shows that the Fourier analysis gives the most similar sea level rising trend of above two stations. The maximum sea level difference rising up to 120mm from other analysis. It is apparently that different analysis methods predict SLR with somewhat inconsistency and uncertainty.

3.3 Discussions of Risk Map

To investigate the coastal flooding in mid-western coastal areas of Taiwan, the integrated coastal-watershed models were employed. The simulations for scenario of the target future were carried out using adaptive grids for the varying topography, and considered the impact of sea level rise, astronomic tide, storm surge, run-up, and overtopping. Based on the standard design of engineering practice, it is acceptable to

adopt the design of the 50-year return periods of wave, and the probability of structure damages within the design year is about 64% (Hsu *et al*, 2015). The comparison of the simulated flooding areas of the status quo (1980–1999) and the target's future (2020–2039) under the climate change scenarios with different return periods of 50 year, 100 year, and 200 year during typhoon attack the study area were conducted. The attack is from east Pacific Ocean to west coast of Taiwan resulting in many flooding. The overall simulation result shows surge tides and overtopping by typhoons of different paths can result in floods of different magnitudes. Estuaries are more prone to bring in much floods. Model results also indicate that the flooding depths are varied from 0.5 m to 0.8m. Simulations show the maximum flooding areas of the status quo (1980–1999), are 4,376, 4,527, and 4600 hectares of the 50-year, 100-yr and 200-yr return period, respectively. For the target's future (2020–2039), they are 6,933, 7,693, 7,812 hectares of the 50-year, 100-yr, and 200-yr return period. In other words, additional 70 % of flooding regions are extended in the future climate effects.

The simulated results also help to produce the hazard maps. These hazard maps together with surveys of artificial facilities, environmental geography and socio-economics, can produce risk maps indicating the risk of different classifications: very low, low, medium, high, and very high. Figure 4 shows the vulnerability of the target's

future (2020–2039) considering surge tides and precipitations with AHP weights (see Table 1). Figure. 4 shows that the risk of most villages or towns is in the range of medium to low; the right one shows that many villages or towns are in medium risk, except that Wuqi, Lukang, Mailiao, and Taixi can reach the high-risk level.

4. Conclusions and Suggestions

The purpose of this research is to assess the impact from coastal disasters under climate change with integrated coastal-watershed models and AHP risk assessment approaches. The assessment of this study focus on the sea level rise, seawall safety, floods, and coastal vulnerability. Mid-western coasts of Taiwan, within the administrative divisions of Taichung City, Changhua County and Yulin County, were illustrated for simulation and analysis.

Simulation results indicated that the sea level at the mid-western coast of Taiwan will rise in an average of 5.8 cm from 2020 to 2039, equivalent to a rising velocity of 2.8 mm/year. The maximum wave typhoon induced height increase about 35.98 % and the maximum typhoon surge deviation will increase 29.15 % as compared to status-quo situation. To assess coastal disaster risks under climate change with AHP weighting mode, Wuqi, Lukang, Mailiao, and Taixi counties reach the high-risk level. Results also showed that the climate change has significant impact on the study area. Several alternatives, e.g. enhancing the monitoring facilities and data accuracy, increasing the

seawall height for areas with higher population density, establishing second seawalls, deploying emergency pumping equipment in areas prone to flooding, and improving disaster response system, etc. are recommended to reduce the loss of lives and properties.

Acknowledgements

This research is founded by the Water Recourses Agency, Ministry of Economic Affairs, Taiwan, under Grant no. MOEA-WRA-1040038.

References

1. Acreman, M., Sinclair, C., 1986. Classification of drainage basins according to their physical characteristics; and application for flood frequency analysis in Scotland. *J. Hydrol.* 84, 365-380.

2. Akhtar, M., Ahmad, N., Booij, M. J., 2008. The impact of climate change on water resources of Hindukush–Karakorum–Himalaya region under different glacier coverage scenarios. *J. Hydrol.* 355, 148-163.

3. Arnell, N. W., Gosling, S.N., 2013. The impacts of climate change on river flow regimes at the global scale. *J. Hydrol.* 486, 351-364.

4. Beven, K., Wood, E., Sivapalan, M., 1988. On hydrological heterogeneity – catchment morphology and catchment response. *J. Hydrol.* 100, 353-375.

5. Beckley, B. D., Lemoine, F. G., Luthcke, S. B., Ray, R. D., Zelensky, N. P., 2007. A reassessment of global and regional mean sea level trends from TOPEX and Jason-1 altimetry based on revised reference frame and orbits. *Geophys. Res. Lett.*, 34(14), L14608.

6. Bilskie, M. V., Hagen, S. C., Alizad, K., Medeiros, S. C., Passeri, D. L., Needham, H., Cox, A., 2016. Dynamic simulation of numerical analysis of hurricane storm surge under sea level rise along the northern Gulf of Mexico. *Earth's Future*, 4(5), 177–193.

7. Bilskie, M.V., Hagen, S.C., Medeiros, S.C., Passeri, D.L., 2014. Dynamics of sea level rise and coastal flooding on a changing landscape. *Geophysical Research Letters*, 41, 1-8.

8. Blumberg, A. F., Mellor, G. L., 1987. A description of a three-dimensional coastal ocean circulation model. *Three-Dimensional Coastal Ocean Models, American Geophysical Union*, Washington, D.C., Vol. 4, edited by N.Heaps, pp.208.

9. Cayan, D. R., Bromirski, P. D., Hayhoe, K., Tyree, M., Dettinger, M. D., Flick, R. E., 2008. Climate change projections of sea level extremes along the California coast. *Clim. Chang*, 87, S57-S73.

10. Chen, X., Alizad, K., Wang, D., Hagen, S. C., 2014. Climate change impact on runoff and sediment loads to the Apalachicola River at seasonal and event scales. *J. Coastal Res.*, 68, 35-42.

11. Déqué, M., Rowell, D. P., Lüthi, D., Giorgi, F., Christensen, J. H., Rockel, B., Jacob, D., Kjellström, E., de Castro, M., van den Hurk, B., 2007. An intercomparison of regional climate simulations for Europe: assessing uncertainties in model projections. *Clim. Change*. 81, 53-70.

12. Doukakis, E., 2005. Coastal vulnerability and risk parameters. *European Water*, 11(12), 3-7.

13. Easterling, D. R., Meehl, G. A., Parmesan, C., Changnon, S. A., Karl, T. R., Mearns,

L. O., 2000. Climate extremes: observations, modeling, and impacts. *Science*, 289(5487), 2068-2074.

14. Guo, S. L., Wang, J. X., Xiong, L. H., Ying, A. W., Li, D. F., 2002. A macro-scale and semi-distributed monthly water balance model to predict climate change impacts in China. *J. Hydrol.* 268 (1–4), 1-15.

15. Harbor and Marine Technology Center, Ministry of Transportation and Communications, 2010, “Long-term Marine Meteorological Observations of Taiwan's Major Harbor Sea Areas and Application of the Data Characteristics 1/4”, Taipei, Taiwan. (in Chinese)

16. Hay, L. E., Markstrom, S. L., Ward-Garrison, C., 2011. Watershed-scale response to climate change through the twenty-first century for selected basins across the United States. *Earth Interact.*, 15(17), 1-37.

17. Hallegatte, S., Green, C., Nicholls, R. J., Corfee-Morlot, J., 2013. Future flood losses in major coastal cities. *Nature Climate Change*, 3, 802-806.

18. Holland, G. J., 1980. An analytical model of the wind and pressure profiles in hurricanes. *Monthly Weather Review*, 108, 1212-1218.

19. Hong, H., Cui, S., Zhang, L., 2006. A coastal vulnerability index and its application in Xiamen, China. *Aquatic Ecosystem Health & Management*, 9(3), 333-337.

20. Hovenga, P. A., Wang, D., Medeiros, S. C., Hagen, S. C., Alizad, K. A., 2016. The

response of runoff and sediment loading in the Apalachicola River, Florida to climate and land use land cover change. *Earth's Future*, 4, 124-142.

21. Hsu, T. W., Shih, D. S., Chen, W. J., 2015. Destructive Flooding Induced by Broken Embankments along Linbian Creek, Taiwan, during Typhoon Morakot. *Journal of Hydrologic Engineering (ASCE)*, 20(7), 05014025-1~05014025-9.
22. Hsu, T. W., Liau, K. M., Lin, J. G., Zheng, J., Ou, S. H., 2011. Sequential assimilation in the wind wave model for simulations of typhoon events around Taiwan Island. *Ocean Engineering*, 38, 456-467.
23. Hsu, T. W., Ou, S. H., Liau, J. M., 2005. Hindcasting nearshore wind waves using a FEM code for SWAN. Coas*tal Engineering*, 52, 177-195.
24. IPPC-CZM, 1991, The Seven Steps to the Vulnerability Assessment of Coastal Areas to Sea-Level Rise – Guideline for case studies. pp. 46.
25. IPCC, Summary for Policymakers, In: Climate Change 2014, Mitigation of Climate Change. Contribution of Working Group III to the Fifth Assessment Report of the Intergovernmental Panel on Climate Change [Edenhofer, O., R. Pichs-Madruga, Y. Sokona, E. Farahani, S. Kadner, K. Seyboth, A. Adler, I. Baum, S. Brunner, P. Eickemeier, B. Kriemann, J. Savolainen, S. Schlömer, C. von Stechow, T. Zwickel and J.C. Minx (eds.)]. Cambridge University Press, Cambridge, United Kingdom and New York, NY, USA (2014).

26. Kavi Kumar K. S. and Tholkappian, S., 2006. Relative vulnerability of Indian coastal districts to sea-level rise and climate extremes. *International Review for Environmental Strategies*, 6(1), 3-22.

27. Kling, H., Stanzel, P., Preishuber, M., 2014. Impact modelling of water resources development and climate scenarios on Zambezi River discharge. *J. Hydrol.*: Reg. Stud., 1, 17–43.

28. Lan, Y. J., Hsu, T. W., Lin, Y. C., Huang, C. J., 2013. An Adaptation Due to Climate Change in Southwest Coast of Taiwan. *Coastal Management*, 41(2), 172-189.

29. Lin, S. C. Tang, T. Y., 2003. Factor Assessment of the Environmental Impact for Tainan Technology Industry Area in Taiwan, In: Ecosystems and Sustainable Development," Volume I, Edited by E. Tiezzi, C. A. Brebbia and J. L. Uso, WIT Press, Boston, pp. 219-229.

30. Mastrandrea, M. D., Luers, A. L., 2012. Climate change in California: scenarios and approaches for adaptation. *Clim. Chang.* 111(1), 5-16.

31. Mellor, G. L., 1998. USERS GUIDE for A THREE-DIMENSIONAL, PRIMITIVE EQUATION, NUMERICAL OCEAN MODEL. Princeton University, Princeton, NJ.

32. Menzel, L., Thieken, A. H., Schwandt, D., Bürger, G., 2006. Impact of climate change on the Regional hydrology – Scenario-based modelling studies in the German Rhine catchment. *Nature Hazards.* 38, 45-61.

33. Minville, M., Brissette, F., Leconte, R., 2008. Uncertainty of the impact of climate change on the hydrology of a Nordic watershed. *J. Hydrol.* 358, 70-83.

34. Nicholls, R. J., 2004. Coastal flooding and wetland loss in the 21st century: changes under the SRES climate and socio-economic scenarios. *Global Environmental Change*, 14(1), 69–86.

35. Nicholls, R. J., 2002. Analysis of global impacts of sea-level rise: a case study of flooding. *Physics and Chemistry of the Earth*, 27, 1455-1466.

36. Nicholls, R. J., Hoozemans, F. M. J., Marchand, M., 1999. Increasing flood risk and wetland losses due to global sea-level rise: regional and global analyses. *Global Environmental Change*, 9, S69–S87.

37. Passeri, D. L., Hagen, S. C., Medeiros, S. C., Bilskie, M. V., Alizad, K., Wang, D., 2015. The dynamic effects of sea level rise on low-gradient coastal landscapes: A review. *Earth's Future*, 3(6), 159-181.

38. Passeri, D. L., Hagen, S. C., Plant, N. G., Bilskie, M. V., Medeiros, S. C., Alizad, K., 2016. Tidal hydrodynamics under future sea level rise and coastal morphology in the Northern Gulf of Mexico. *Earth's Future*, 4(5), 159-176.

39. Prudhomme, C., Davies, H., 2008. Assessing uncertainties in climate change impact analyses on the river flow regimes in the UK. Part 2: future climate. *Clim. Change*. 93, 177–195.

40. Rahmstorf, S., 2007. A Semi-Empirical Approach to Projecting Future Sea-Level Rise. *Science*, 315 (5810), 368-370.

41. Scavia, D., Field, J. C., Boesch, D. F., Buddemeier, R. W., Burkett, V., Cayan, D. R., Fogarty, M., Harwell, M. A., Howarth, R. W., Mason, C., Reed, D. J., Royer, T. C., Sallenger, A. H., Titus, J. G., 2002. Climate Change Impacts on US Coastal and Marine Ecosystems, *Estuaries*, 25 (2), 149-164.

42. Shih, D. S., T. W. Hsu, K. C. Chang and Juan H. L., 2012. Implementing Coastal Inundation Data with an Integrated Wind Wave Model and Hydrological Watershed Simulations. *Terrestrial Atmospheric and Oceanic Sciences*, 23(5), 513-525.

43. Small, C., and Nicholls, R.J., 2003. A global analysis of human settlement in coastal zones. *Journal of Coastal Research*, 19, 584–599.

44. Small, C., Gornitz, V., Cohen, J. E., 2000. Coastal hazards and the global distribution of human population. *Environmental Geosciences*, 7, 3-12.

45. Stefanidis S., Stathis D., 2013. Assessment of flood hazard based on natural and anthropogenic factors using analytic hierarchy process (AHP). *Nature Hazards*. 68, 569-585.

46. Taiwan Climate Change Projection and Information Platform Project (TCCIP), http://tccip.ncdr.nat.gov.tw/v2/index_en.aspx.

47. Tehrany M. S, Pradhan, B., Jebur, M. N., 2014. Flood susceptibility mapping using a novel ensemble weights-of-evidence and support vector machine models in GIS. *J Hydrol.* 512, 332-343.

48. United Nations Disaster Relief Co-ordinator (UNDRO), 1980, "Natural disasters and vulnerability analysis : report of Expert Group Meeting (9-12 July 1979)," Geneva, Switzerland.

49. United Nations Environment Programme Report (UNEP), "Assessing Coastal Vulnerability: Developing a Global Index for Measuring Risk", http://www.unep.org/ (2005).

50. Veijalainen, H., Lotsari, E., Alho, P., Vehviläinen, B., Käyhkö, J., 2010. National scale assessment of climate change impacts on flooding in Finland. *J. Hydrol.* 391(3-4), 333-350.

51. Wu, L. C., Kao, C. C. Hsu, T. W. Jao, K. C. Wang, Y. F., 2011. Ensemble empirical mode decomposition on storm surge separation from sea level data. *Coastal Engineering Journal*, 53(3), 223-243.

52. Yan, D., Werners, S. E., Ludwig, F., Huang, H. Q., 2015. Hydrological response to climate change: The Pearl River, China under different RCP scenarios. *J. Hydrol.* 4, Part B, 228-245.

53. Yeh, G. T., Huang, G. B., Zhang, F., Cheng, H. P., Lin, H. C, 2006. WASH123D: A

Numerical Model of Flow, Thermal Transport, and Salinity, Sediment, and Water Quality Transport in WAterSHed Systems of 1-D Stream-River Network, 2-D Overland Regime, and 3-D Subsurface Media. *Technical Rep. Submitted To EPA*, Dept. of Civil and Environmental Engineering, University of Central Florida, Orlando, Florida.

54. Yeh, G. T., Shih, D. S. Cheng, J.R. C., 2011. An Integrated Media, Integrated Processes Watershed Model. *Computers and Fluids,* 45, 2-13.

1 Table 1. The structures and weights of the coastal risk analysis based on the AHP evaluation

Aspect		Construction		Index	
Aspect	Weight	Construction	Weight	Index	Weight
Hazzard potential	0.404	Hazard factors	1.000	The range of flooding overflow	0.384
				The depth of flooding overflow	0.271
				The range of surging tide overflow	0.159
				The depth of surging tide overflow	0.186
Vulnerability	0.596	Artificial facilities	0.327	Seawall relative length	0.257
				Seawall relative height	0.499
				Tidal gate relative comparison	0.244
		Environmental geography	0.548	Elevation	0.139
				Slope	0.098
				Tide range	0.086
				Coastal erosion rate	0.226
				Land subsidence rate	0.359
				Land use	0.093
		Social economy	0.125	Population density	0.415
				Education background	0.223
				Dependency ratio	0.166
				Enterprise return	0.196

2

3 Table 2. Maximum typhoon induced wave heights of different return periods for the target's future.

Return Period of Typhoon Wind Waves (in years) / Coastal Areas (Longitude, Latitude)	Status quo (2014)			Target year (2020-2039)		
	50-yr	100-yr	200-yr	50-yr	100-yr	200-yr
Da-an River (120.5604°, 24.4193°)	6.99	6.90	7.10	8.94	9.43	9.48
Taichung (Taichung Harbor) (120.4719°, 24.29778°)	6.82	7.02	7.20	9.16	9.65	9.67
Wu River (120.3859°, 24.2151°)	6.79	7.00	7.19	9.68	10.10	10.34
Changhua (south side of Chabnghua Coastal Industrial Park) (120.2761°, 24.06278°)	7.09	7.34	7.57	9.45	10.01	10.09
Jhuoshuei River (120.1514°, 23.8818°)	7.40	7.91	8.42	10.38	11.35	12.08
Yulin (Shantiaolun) (120.0594°, 23.70583°)	6.79	6.99	7.17	8.52	8.82	9.55
Beigang River (119.9902°, 23.5403°)	7.20	7.47	7.80	9.67	10.27	10.59

4 Note: Unit in meters (m). The recommended range is within the 10km radius area along the coasts. Its cycle is calculated by $\mathbf{4.14}\sqrt{\mathbf{wave\ \ height}}$ (Harbor and
5 Marine Technology Center, Ministry of Transportation and Communications, 2010).

6 Table 3. Maximum storm surge deviations of different return periods for the target's future

Return Period of Typhoon Wind Waves (in years) / Coastal Areas (Longitude, Latitude)	Status quo (2014)			Target year (2020-2039)		
	50-yr	100-yr	200-yr	50-yr	100-yr	200-yr
Da-an River (120.5604°, 24.4193°)	1.27	1.37	1.45	1.52	1.62	1.65
Taichung (Taichung Harbor) (120.4719°, 24.29778°)	1.14	1.22	1.29	1.41	1.49	1.55
Wu River (120.3859°, 24.2151°)	1.00	1.07	1.13	1.28	1.37	1.36
Changhua (south side of Chabnghua Coastal Industrial Park) (120.2761°, 24.06278°)	1.00	1.05	1.09	1.29	1.30	1.44
Jhuoshuei River (120.1514°, 23.8818°)	1.05	1.13	1.19	1.32	1.45	1.46
Yulin (Shantiaolun) (120.0594°, 23.70583°)	0.90	0.99	1.09	1.17	1.37	1.4
Beigang River (119.9902°, 23.5403°)	0.76	0.84	0.92	1.04	1.15	1.24

7 Unit: m

8

9 Table 4. The amount of overtopping of different return periods at different places for the target's future

	Target year (2020-2039)				
	5-yr	50-yr	100-yr	200-yr	250-yr
The Dinggueike seawall at Da-an District, Taichung City	0.000	0.020	0.031	0.040	0.057
The Shinjie seawall at Fangyuan Township, Changhua County	0.000	0.010	0.015	0.025	0.030
The Dacheng seawall at Dacheng Township, Changhua County	0.000	0.000	0.001	0.003	0.004
The Lintsouliao seawall at Sihu Township, Yulin County	0.000	0.011	0.026	0.039	0.059

10 Unit: cms/m

11

12 Table 5. Estimation of average sea level rise in mid-western coast of Taiwan

Tidal Gauge Station	Analysis Base Period (year)	Fourier Analysis	Ensemble Empirical Model Decomposition (EEMD)	Average Amount of Change
Taichung Harbor (120.25°E, 24.25°N)	1980–1999	40	68	54
Jiayi Dongshi (119.75°E, 23.25°N)	1992–2013	43	81	62

13 Unit: mm

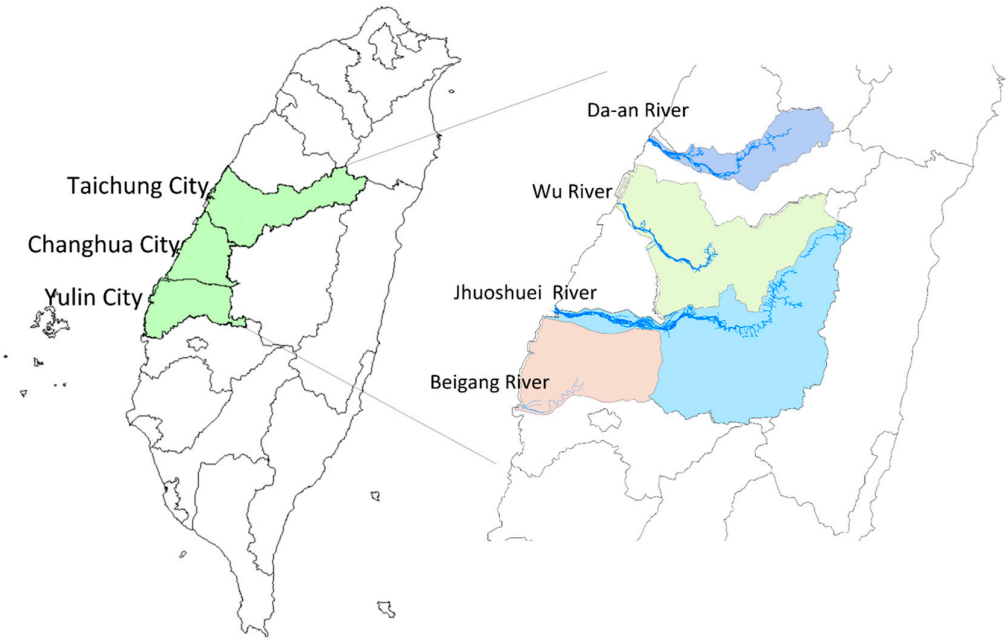

Fig. 1. Study areas in mid-western coast of Taiwan in including Taichung City,

Changhua County and Yulin County.

Preprints (www.preprints.org) | NOT PEER-REVIEWED | Posted: 21 March 2017 doi:10.20944/preprints201703.0172.v1

Peer-reviewed version available at Water 2017, 9, , 390; doi:10.3390/w9060390

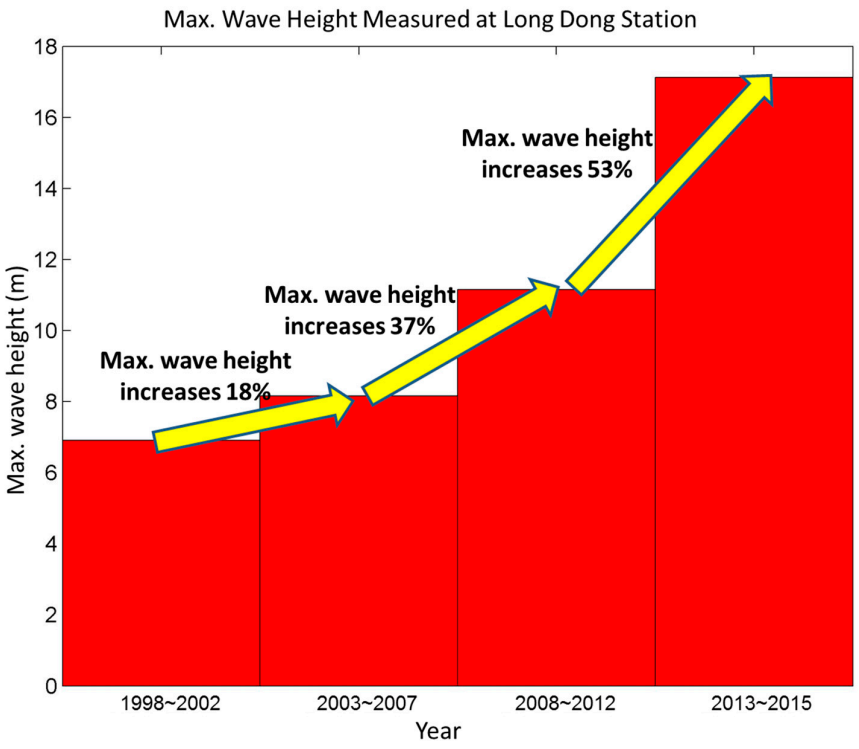

Fig. 2. Increasing trend of maximum wave height measured at Long Dong station located at northeast coast of Taiwan

Preprints (www.preprints.org) | NOT PEER-REVIEWED | Posted: 21 March 2017 doi:10.20944/preprints201703.0172.v1

Peer-reviewed version available at Water 2017, 9, , 390; doi:10.3390/w9060390

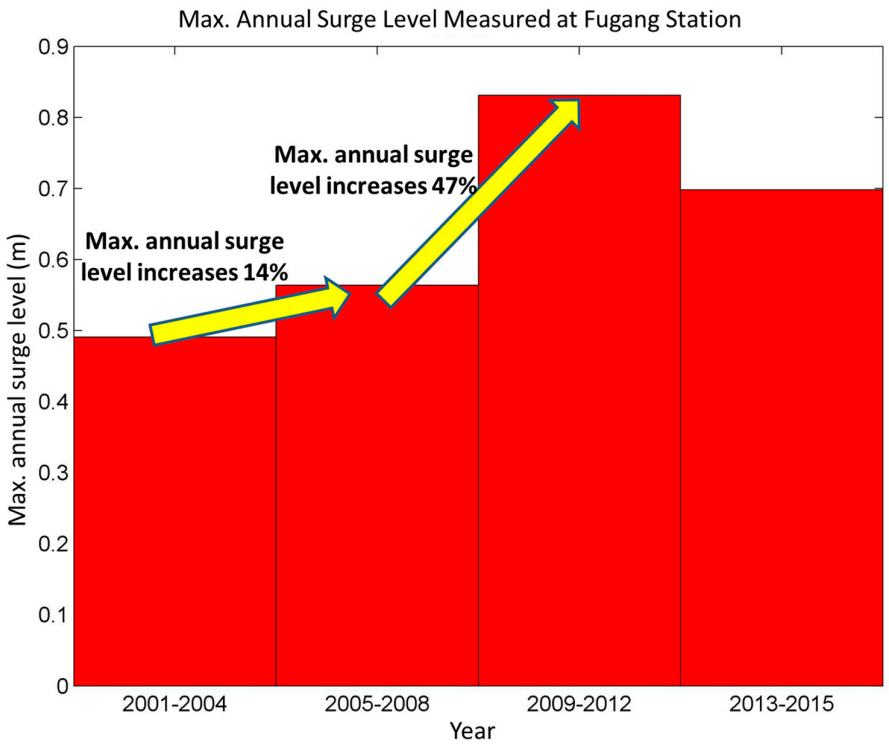

Fig. 3. Increasing trend of maximum annual surge level measured at Fugang station located at southeast coast of Taiwan

Preprints (www.preprints.org) | NOT PEER-REVIEWED | Posted: 21 March 2017 doi:10.20944/preprints201703.0172.v1

Peer-reviewed version available at Water 2017, 9, , 390; doi:10.3390/w9060390

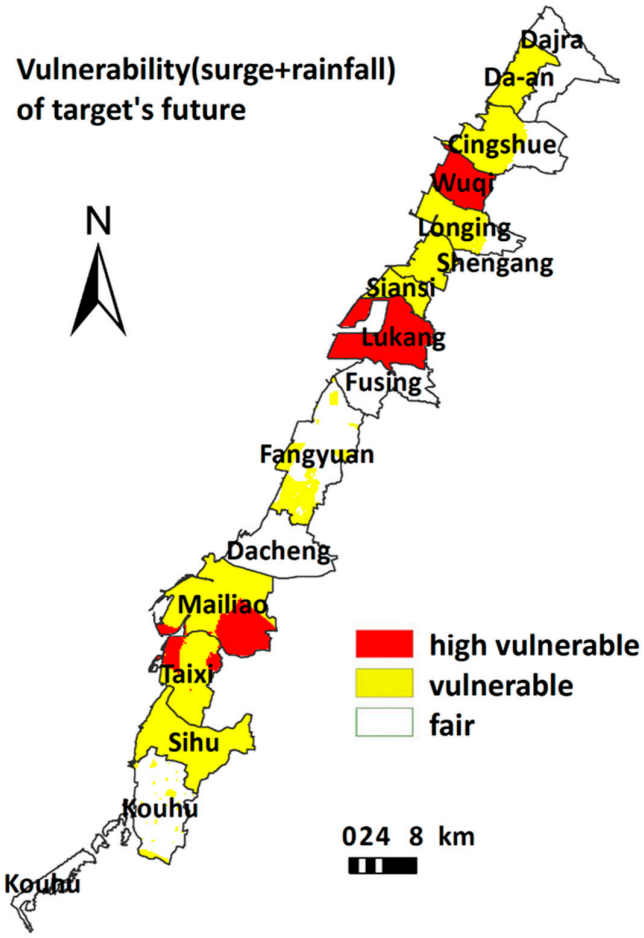

Fig. 4. Vulnerability map of target's future (2020-2039) with considering surge tides and precipitations using AHP weights.